Chemosphere 300 (2022) 134499

Contents lists available at ScienceDirect

Chemosphere

journal homepage: www.elsevier.com/locate/chemosphere

Composite waste recycling: Predictive simulation of the pyrolysis vapours and gases upgrading process in Aspen plus

A. Serras-Malillos *, E. Acha, A. Lopez-Urionabarrenechea, B.B. Perez-Martinez, B.M. Caballero

Chemical and Environmental Engineering Department, Faculty of Engineering of Bilbao, University of the Basque Country (UPV/EHU), Plaza Ingeniero Torres Quevedo, 1, 48013, Bilbao, Spain

HIGHLIGHTS

- Kinetic multi-reaction model is proposed for pyrolysis vapours and gases upgrading.
- Simulations confirm the reduction of the number of compounds at the outlet stream.
- 95 vol% of syngas is thermodynamically predicted at 900 °C.
- Kinetic prediction for H_2 (g) at 900 °C has a 3.8 vol% absolute error.

GRAPHICAL ABSTRACT

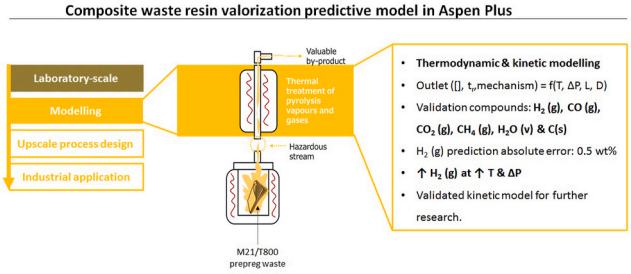

ARTICLE INFO

Handling Editor: Derek Muir

Keywords:
Composite waste recycling
Carbon fiber reinforced polymer
Epoxy resin valorisation
Predictive process modelling
Aspen plus
Circular economy

ABSTRACT

Waste generation is one of the greatest problems of present times, and the recycling of carbon fibre reinforced composites one big challenge to face. Currently, no resin valorisation is done in thermal fibre recycling methods. However, when pyrolysis is used, additional valuable compounds (syngas or H_2-rich gas) could be obtained by upgrading the generated vapours and gases. This work presents the thermodynamic and kinetic multi-reaction modelling of the pyrolysis vapours and gases upgrading process in Aspen Plus software. These models forecast the theoretical and in-between scenario of a thermal upgrading process of an experimentally characterised vapours and gases stream (a blend of thirty-five compounds). Indeed, the influence of temperature (500 °C–1200 °C) and pressure (ΔP = 0, 1 and 2 bar) operating parameters are analysed in the outlet composition, residence time and possible reaction mechanisms occurring. Validation of the kinetic model has been done comparing predicted outlet composition with experimental data (at 700 °C and 900 °C with ΔP = 0 bar) for H_2 (g), CO (g), CO_2 (g), CH_4 (g), H_2O (v) and C (s). Kinetic and experimental results show the same tendency with temperature, validating the model for further research. Good kinetic fit is obtained for H_2 (g) (absolute error: 0.5 wt% at constant temperature and 0.3 wt% at variable temperature) and H_2O (v) shows the highest error at variable T (8.8 wt%). Both simulation and experimental results evolve towards simpler, less toxic and higher generation of hydrogen-rich gas with increasing operating temperature and pressure.

* Corresponding author.
E-mail address: adriana.serras@ehu.eus (A. Serras-Malillos).

https://doi.org/10.1016/j.chemosphere.2022.134499
Received 25 December 2021; Received in revised form 25 February 2022; Accepted 31 March 2022
Available online 4 April 2022

1. Introduction

There is no denial that circular economy is an effective strategy to reduce waste. The challenge is to implement this concept with complex waste, such as composite materials. The outstanding material properties of carbon fibre reinforced polymers (CFRP) make them to be widely used in many industries such as defence, aeronautic, energy and automotive. So far, about the 23% of the current carbon fibre (CF) demand corresponds to the aeronautic sector (Zhang et al., 2020). This industry has progressively increased the use of composites in the manufacturing of planes, having reached 50 and 52 wt% in the Boeing 737 (Hale, 2012) and Airbus A350 (Marsh, 2010) plane models, respectively. Moreover, carbon fibre is also consolidating its presence in the automotive sector, due to continuous improvements in the automation of manufacturing processes. In this case, the driving force is the advantage provided by the very lightweight of the composites, having a direct effect in the reduction of emissions in vehicles. As a result, composite waste generated during the manufacturing processes, as well as at the end of their lifespan, will continue increasing in the coming years. In fact, when the planes manufactured between 2010 and 2020 reach their end of life, the aeronautic sector is expected to produce 9540 t of CFRP waste/year between 2020 and 2035 and 23,360 t of CFRP waste/year in the period 2035–2050 (Lefeuvre et al., 2017). Therefore, there is an urgent need to implement a circular economy model to recover carbon fibres from waste, and reintroduce them as secondary raw materials in fibre-consuming sectors, although currently there is no specific regulation for this waste.

In recent years, significant research is being done towards the reclamation of carbon fibres from waste composites. Among the existing recycling processes, thermal ones, such as pyrolysis, have the highest technology readiness level (TRL), followed by solvolysis and biological degradation. Nowadays, the existing composite waste recycling companies, such as Gen 2 Carbon, Karborek RCF and Reciclalia (Bueno Lopez et al., 2017) among others, focus only on the carbon fibre reclamation and do not valorise the resin, which evolves into a complex condensate that would probably be classified as hazardous waste according to its composition. A patented research carried out by the authors of this work shows that valuable chemical compounds, such as syngas or hydrogen, could be recovered from the vapours and gases generated in the pyrolysis process of waste composite if an appropriate thermal-catalytic treatment is implemented to upgrade them (López Urionabarrenechea et al., 2016). However, it is still needed to work on the up-scale of this process prior to its integration in the existing waste composite recycling processes. Among others, process-modelling tools are required to bridge the gap between laboratory and industrial implementation. The scientific work required to implement the resin valorisation process in carbon fibre recycling industries would be a significant breakthrough, as it would transform a hazardous waste into a safer and saleable by-product. Nevertheless, the successful reactor upscale would depend on the adequate configuration, sizing and choice of the process operating conditions. In this sense, there is one major limitation with size specific parameters, as optimum operating conditions at laboratory-scale would not necessarily be valid for a pilot or industrial scale. Even though reactor simulation may not provide highly precise prediction of its performance, it could give qualitative guidance for design and operation, meaning it can assist in the scale-up design from one successfully operating size to another (Basu, 2018).

The added value of the upgrading process studied in this work is the generation of hydrogen-rich gas from a complex vapours and gases mixture. Therefore, the generation of this gas will be the key parameter indicator in the upscale design process, and hence, in the simulation process. The strategy adopted for this work is to model the chemical transformation occurring during the resin valorisation process with Aspen Plus software (Aspen Technology Inc., 2021). Outlet gas stream composition is predicted in function of inlet stream composition, reactor temperature, pressure and basic geometric dimensions. The simulation is fed and validated with experimental own data. The significance of developing such a predictive model is twofold: I) to gain a better understanding of the reactions occurring during the upgrading process and the influence of process parameters (temperature and pressure) in the composition of outlet vapours and gases, and II) its availability for integration with fluid dynamics and heat transfer simulation models to evaluate the impact of process dimensions at the outlet gas composition in a subsequent research stage.

Until now the goal of the majority of the simulation research works, related to composite materials, has been to better understand and predict the response of CFRP materials in the presence of fire (Grange et al., 2018; McKinnon et al., 2017; Stoliarov et al., 2014; Tranchard et al., 2015, 2017a, b, c). However, the emphasis of the kinetic models proposed by these research groups lays on the weight loss, more than in the specific chemical decomposition reactions. Notwithstanding the relevance of existing thermal degradation simulation studies for epoxy based composites, no predictive modelling has been found in the literature in terms of chemical compounds generation. Neither was found on the products generated during secondary cracking that undergo pyrolysis vapours and gases when a subsequent thermal degradation process is applied, as is the case of the technology patented by the authors.

Moreover, even though many pyrolysis simulation works have been carried out using Aspen Plus software for biomass feedstock, no modelling concerning CFRP pyrolysis or thermal treatment of the pyrolysis vapours and gases was found. Although those works are focused on biomass, adopted modelling strategies could be of interest. Indeed, according to a recent review (Mutlu and Zeng, 2020) and other studies (Gao et al., 2021; Salisu et al., 2021), the most common adopted strategies and assumptions include: 1) equilibrium and kinetic approaches, 2) steady state regime, 3) isothermal homogeneous temperature and pressure profile, 4) no pressure drops, 5) no tar consideration or representation by model compounds, and 6) model validation based on literature data in terms of obtained syn-gas composition. Indeed, regarding pyrolysis vapours upgrading process, A. Ahmed et al. (2015) reviewed the principal tar formation and removal (by reforming or cracking) modelling strategies in biomass thermal treatment using Aspen Plus software. In the reviewed works (Damartzis et al., 2012; De Kam et al., 2009; Francois et al., 2013; Hannula and Kurkela, 2012; Nilsson et al., 2012; Panopoulos et al., 2006; Sadhukhan et al., 2010), tar is represented by model compounds (naphthalene, toluene, benzene and phenol) varying from one to four species depending on the study.

The present work aims to develop a pyrolysis vapours and gases upgrading model in Aspen Plus by using experimental own data to validate its applicability in the up-scale process optimisation design for an epoxy based CFRP waste. More precisely, thermodynamic and kinetic reactor models are used fed by experimental data generated at laboratory scale, and constant and variable temperature and pressure drop scenarios are studied. Moreover, vapours and gases thermal upgrading is modelled kinetically with a simplified fifteen compound stream, including three model-compounds to represent oxygen, sulphur and nitrogen aromatics. Model validation is done comparing data related to the generation tendencies (in wt%) for main gaseous species (H_2 (g), CO (g), CO_2 (g), CH_4 (g)), water vapour and solid carbon for experimental and simulation results. Absolute error (difference between experimental and simulated results) of the predicted results is also calculated.

2. Materials and methods

2.1. Experimental data for the simulation

The yield and composition of the vapours, gases and solid carbon at the inlet and outlet of the vapours and gases treatment reactor was needed to run the thermodynamic and kinetic simulations. On the one hand, to determine the inlet composition, pyrolysis of 100 g of an expired carbon fibre reinforced epoxy pre-preg composite (T800/M21) was carried out in a non-stirred tank reactor by heating the sample at

3 °C min^{-1} up to 500 °C in the absence of any carrier gas. In such conditions 20.2 g of vapours + gases and 79.8 g of solid (reclaimed carbon fibres 66 g and char 13.8 g, assumed as 100 wt% solid carbon) were obtained. The composition of vapours (collected as liquids) and gases were analysed by gas chromatography (GC AGILENT 6890, United States) coupled with mass spectrometer detector (MS AGILENT 5973, United States) and gas chromatography (AGILENT 7890A, United States) coupled with thermal conductivity detector (TCD) and flame ionization detector (FID), respectively. The composition of the gases was calibrated using a standard refinery gas mixture, while in the case of liquids (condensed vapours), area percentage obtained at the GC-MS was assumed to equal weight percentage, due to the complexity of the composition. In addition to the mentioned analytical techniques, Fourier transform infrared (FTIR) DX-4000 model gas analyser (Gasmet, Finland) was also used to qualitatively identify trace compounds. Further details of the pyrolysis laboratory installation are described elsewhere (Lopez-Urionabarrenechea et al., 2021).

On the other hand, the composition of vapours, gases and solid carbon at the outlet of the treatment reactor was determined by carrying out experiments where pyrolysis of the expired pre-preg took place at the same conditions described above and the generated pyrolysis vapours and gases ascending by natural convection passed through a fixed bed tubular reactor (treatment reactor), to be upgraded at 700 °C and 900 °C. Material of the fixed bed treatment reactor is stainless steel (AISI-309), dimensions are 0.6 m long and a 0.02 m inner diameter and it is electrically and concentrically heated. The reactor was filled with refractory brick material of 0.5–1 mm particle diameter as solid bed.

The composition of vapours (condensed into liquids) and gases evolving from the treatment reactor was analysed by the same chromatographic methods described previously. Some chemicals were not well identified by the MS library when analysing liquids coming from vapours condensation composition determination. To feed the simulation, this percentage of unidentified compounds at both, inlet (12 wt%) and outlet (16 wt% at 700 °C and 4 wt% at 900 °C), was proportionally distributed among the well-identified compounds to specify the composition of the streams under study. Additionally, six compounds found in vapours (1,3-benzothiazole, 1-methyl-3-phenoxybenzene, phenylsulfanybenzene, 6H-benzo[c]chromene, 5-methyl-1H-indole, 2,3-dimethyl-1H-indole) were excluded from the simulation due to the problems they pose in Aspen Plus v11 blocks because of missing properties and/or inadequately estimated properties. Fig. 1 shows the vapours, gases and solid carbon composition (in wt% and vol%) used as inlet and outlet (at 700 °C and 900 °C operating temperatures) streams to be employed and compared with the treatment reactor simulations. The exact weight percentages for each compound and experimental condition shown in Fig. 1 are included in the Supplementary Information (SI) document, in Table S1. Traces of sulphur dioxide, nitrous oxide, ammonia, hydrochloric acid, hexane and formaldehyde were also identified in gas phase by FTIR, but due to lack of quantification they were not included in the simulation. Finally, the fraction of solid carbon generated during the experiments and the fraction of non-recoverable condensed vapours along the walls of the reactors is also included in Fig. 1. Schematic representation of experimentally generated fractions and yield calculation appear in Figure S1-S6 and Table S2-S3.

Apart from vapours and gases, carbon coming from carbonization reactions (assumed as 100% solid carbon) is also a by-product of the upgrading process and it is formed and retained in the particles forming the solid bed of the treatment reactor. Consequently, the solid bed material was characterised in fresh and after-experiment conditions. In the last case, samples extracted from three zones of the treatment reactor were analysed: low, medium and high. Characterization included different analysis: measuring weight gain after experiments, weight loss by calcination at 500 °C, proximate analysis (humidity, volatile matter, fixed carbon and ashes) using LECO TGA-701 (United States) and ultimate analysis using LECO TrueSpec CHNS automatic analyser (United States). The weight gain for the fixed bed material ascended to 3.3 g at 700 °C and 2.9 g at 900 °C, respectively, and an increase in wt% was appreciated for the fourth analysed elements, CHNS. See Table S4, Table S5, Table S6 and Table S7 in SI for further details about the results of fixed bed material characterization.

At last, the kinetic modelling in Aspen Plus offers the possibility of establishing a temperature gradient along the length of the treatment reactor. With that objective, temperature distribution along the reactor was measured with a 600 mm length thermocouple (extracting it 1 cm each time from the upper part of the reactor) using water vapour (0.02 mol/min fed through a Gilson pump) as representative fluid of the pyrolysis vapours for the two studied setpoint temperatures at steady state conditions. The majority (central part) of the reactor length was at constant temperature, while the inlet and outlet sections showed a temperature gradient which was highest at 900 °C and lowest at 700 °C. Details on temperature distribution are shown in Figure S7.

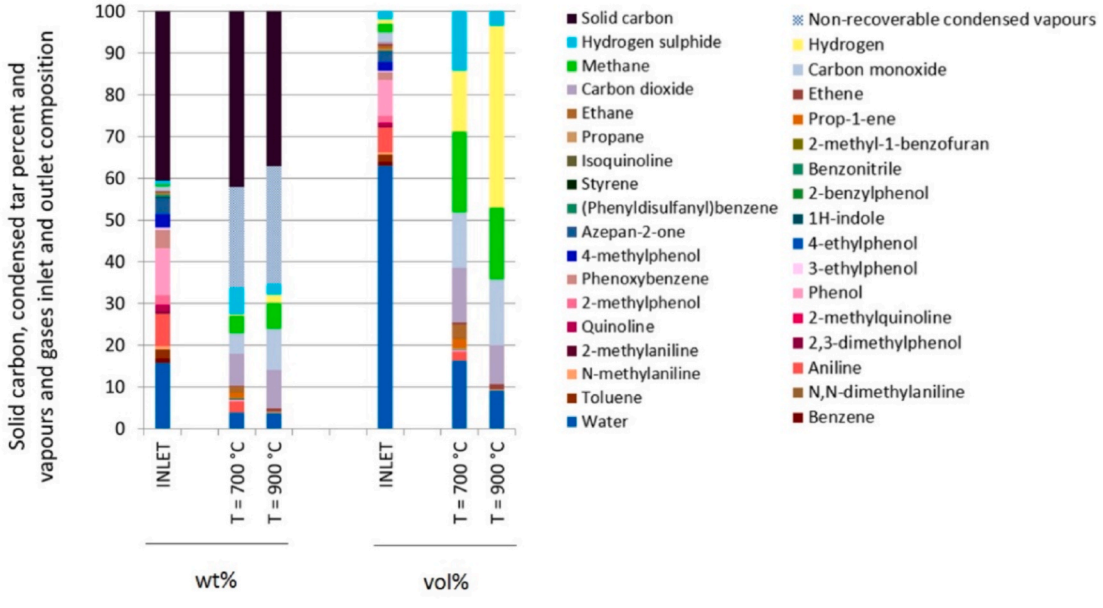

Fig. 1. Vapours and gases composition, solid carbon and condensed tar at the inlet/outlet of the treatment reactor in WT% and vol%.

2.2. Process simulation

The pyrolysis vapours and gases upgrading process is represented in Aspen Plus as indicated in "step 2 upgrading" in the flowsheet diagram shown in Fig. 2, where the conceptualization of an integral waste composite recycling process is shown. For the simulation in Aspen Plus v11, property method selected was Soave-Redlich-Kwong-Kabadi-Danner (SRK-KD), which is adequate for water and hydrocarbon mixtures in the presence of light gases (see details of the model and the equation of state in the SI document in pages 8–9). Regarding model assumptions, simulation regime was set as steady state.

Inlet stream for the PYRO reactor, where the pyrolysis of the expired pre-preg (PRE-PREG) is carried out, was set at a mass rate of 100 g/h, equal to the mass introduced in the laboratory experiments per test run (g/test), and the outlet stream (PYRO-OUT) comprised the generated pyrolysis vapours and gases (VAP + GAS) at a rate of 20.2 g/h and the pyrolysed solid (PYRO-SOL) at a rate of 79.8 g/h (66 g/h of reclaimed carbon fibre and 13.8 g/h of char defined as solid carbon), which are the yields obtained in the lab-scale pyrolysis experiments (see Table S2).

The thermodynamically predicted vapours and gases composition obtained at the outlet of the treatment reactor (V + G-OUT1) was simulated by a thermodynamic model reactor RGibbs (RTHERM), whose calculations are based on the minimization of Gibbs free energy of the chemical system involved. Consequently, it is not the chemical reactions that need to be defined but the chemical system which, in this case, is the one composed by the chemicals experimentally identified in both the reactor inlet and outlet streams. A wide operating temperature range (500 °C–1200 °C) was simulated, which embraces the experimental ones, at 1 bar (absolute pressure) to evaluate possible tendencies in function of temperature. Simulation was performed on the basis of chemical and phase equilibrium calculations.

Concerning the global thermal decomposition kinetic modelling, the vapours and gases outlet composition (V + G-OUT2) including solid carbon was predicted based on the reactor model RPlug (RKIN). This latter approach was meant to provide a more realistic scenario as reactor real dimensions (see section 2.1) and various global thermal decomposition and other typical kinetic reactions of the pyrolysis environment (Table 1) of a simplified solid carbon, vapours and gases stream, were specified. The compilation of these kinetic reactions were chosen by the authors of this work, as representative of the thermal treatment presented and extracted from literature, where the reaction stoichiometry and kinetic parameters information (activation energy, frequency factor and reaction order) was available. Regarding the operating temperature (700 °C, 800 °C and 900 °C), the simulated temperature range focused on previous own research experiments (Gastelu Otazua, 2020) and the simulations were defined considering two scenarios. Firstly, it was assumed the ideal situation where the temperature along the whole treatment reactor was constant and, secondly, a more realistic scenario was simulated by integrating the experimentally measured gradient temperature along the fix bed treatment reactor (see section 2.1). Besides, the influence of pressure was also analysed to determine what the effect of a possible generation of pressure drop in the treatment reactor caused by the fixed bed material could be. On the basis of own experimental observation in the laboratory-scale pilot plant, three different inlet pressures were defined (1 bar, 2 bar and 3 bar), which could be close to reality, while outlet pressure was maintained at 1 bar. Therefore, three pressure drop scenarios were studied: $\Delta P = 0$ bar, $\Delta P = 1$ bar and $\Delta P = 2$ bar.

As far as the authors are concerned, in the literature there is not kinetic data related to the thermal decomposition of each of the chemical compounds identified in the vapours and gases mixture (VAP + GAS) stream. This data research process has mainly, but not exclusively, been done accessing the NIST Chemical Kinetics Database (Manion et al., 2013). Due to this fact, a simplified fifteen compound stream was defined (V + G-IN2) as representative of the whole vapours, gases and solid carbon composition: solid carbon (40.6 wt%), water (15.2 wt%), benzene (1.02 wt%), toluene (3.05 wt%), pyrrole (14.4 wt%), phenol (22.5 wt%), propane (0.09 wt%), prop-1-ene (0.16 wt%), ethane (0.24 wt%), ethene (0.20 wt%), methane (0.46 wt%), carbon dioxide (0.29 wt %), carbon monoxide (0.87 wt%), hydrogen sulphide (0.89 wt%) and hydrogen (0.03 wt%). Indeed, three model-compounds (pyrrole, phenol and toluene) represented the nitrogenous, oxygenated aromatic and sulphur aromatic compounds, respectively.

It should be noted that pyrrole was not present among the experimentally identified species, but it was selected as a representative compound for nitrogenous aromatics in the absence of kinetic information regarding the nitrogenous compounds identified in the performed experimental work. Thus, the prepared model assumes that the cracking mechanism of pyrrole is representative of the nitrogenous species present in the feeding stream, which could differ to a certain extent from reality. Likewise, the kinetic parameters of the thermal decomposition of any of the experimentally observed aromatic sulphur

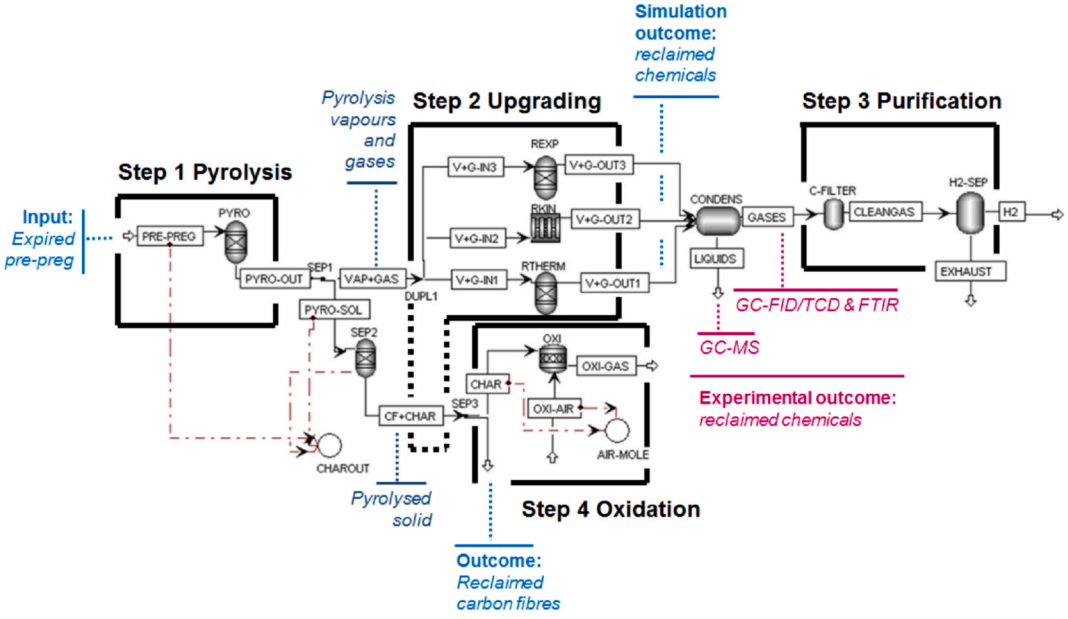

Fig. 2. Flowsheet of the process modelled in Aspen Plus v11.

Table 1
Thermal decomposition kinetic modelled reactions, rate of the reactions and kinetic parameters.

	Thermal decomposition kinetic reaction	- r kmol·m^{-3}·s^{-1}, atm·s^{-1}	E_a (kJ· kmol^{-1})	A (s^{-1}, m, kmol, atm)	Ref
R-1	C_6H_6 (g) + H_2O (g) → 3 C (s) + 2·CH_4 (g) + CO (g)	$k \cdot C^{1.3}_{[C6H6]} \cdot C^{0.2}_{[H2O]}$	443,000	$4.00 \cdot 10^{16}$	Abdelouahed et al., (2012)
R-2	C_7H_8 (g) + H_2 (g) → C_6H_6 (g) + CH_4 (g)	$k \cdot C^{1}_{[C7H8]} \cdot C^{0.5}_{[H2]}$	247,000	$1.04 \cdot 10^{12}$	Abdelouahed et al., (2012)
R-3	C_4H_4NH (g) → CH_4 (g) + 2 C (s)[a] + HCN (g)	$k \cdot C^{1}_{[C4H4NH]}$	311,000	$7.19 \cdot 10^{13}$	Bruinsma et al., (1988)
R-4	C_6H_6O (g) → CO (g) + 0.4·$C_{10}H_8$ (g) + 0.15·C_6H_6 (g) + 0.1·CH_4 (g) + 0.75·H_2 (g)	$k \cdot C^{1}_{[C6H6O]}$	100,000	$1.00 \cdot 10^{7}$	Abdelouahed et al., (2012)
R-5	C_3H_8 (g) → C_3H_6 (g) + H_2 (g)	$k \cdot C^{1}_{[C3H8]}$	234,000	$1.27 \cdot 10^{12}$	Benson, (1967)
R-6	C_3H_6 (g) → C_3H_4 (g) + H_2 (g)	$k \cdot C^{1}_{[C3H6]}$	297,000	$5.01 \cdot 10^{12}$	Barbé et al., (1996)
R-7	C_2H_6 (g) → C_2H_4 (g) + H_2 (g)	$k \cdot C^{2}_{[C3H8]}$	343,000	$1.15 \cdot 10^{-7}$	Brodsky et al., (1960)
R-8	C_2H_4 (g) → C_2H_2 (g) + H_2 (g)	$k \cdot C^{1}_{[C2H4]}$	318,000	$1.8 \cdot 10^{13}$	Towell and Martin, (1961)
R-9	CH_4 (g) → C (s) + 2H_2 (g)	$k \cdot C^{1}_{[CH4]}$	370,000	$6.60 \cdot 10^{13}$	Rodat et al., (2009)
R-10	CO (g) + H_2O (g) → CO_2 (g) + H_2 (g)	$k \cdot C^{1}_{[CO]} \cdot C^{1}_{[H2O]}$	102,400	$1.35 \cdot 10^{5}$	Abdelouahed et al., (2012)
	CO_2 (g) + H_2 (g) → CO (g) + H_2O (g)	$k \cdot C^{1}_{[CO2]} \cdot C^{0.5}_{[H2]}$	318,000	$1.20 \cdot 10^{10}$	Abdelouahed et al., (2012)
R-11	$C_{10}H_8$ (g) → 9 C (s) + (1/6)C_6H_6 (g) + (7/2)H_2 (g)	$k \cdot C^{1.6}_{[C10H8]} \cdot C^{-0.5}_{[H2]}$	350,000	$3.40 \cdot 10^{14}$	Abdelouahed et al., (2012)
R-12	C (s) + β·H_2O (v) → (2-β)·CO_2 (g) + (β-1)·CO (g) + β·H_2 (g) Choice: β = 1.5	$k \cdot P^{1}_{[H2O]}$	240,000[b]	18412.1	Gao et al., (2021)

[a] Hypothesis: 2 C (s) generation instead of C_2 (g).
[b] Ea has been adjusted in order to better adjust the reaction mechanism to experimental observations.

compounds were not found. In this case, a different strategy was implemented. Taking into account the study carried out by Xu et al. (2004) it was assumed that aromatic sulphur compounds crack into toluene and sulphur radical species. This is the reason why, in the present work, the weight percentage associated to those sulphurous compounds was included in the group represented by the model compound toluene. Finally, water weight percentage in the thermodynamic simulation (Table S8) does not exactly equal the one indicated here, because in the kinetic model compounds were proportionally redistributed only due to the exclusion of the weight percentage associated with the unknown species. Therefore, the defined multi-reaction system consists of twelve power-law kinetic reactions, shown in Table 1, associated to the compounds present in the simplified stream (R-1 to R-10 and R-12) and one intermediate specie (R-11) generated as products of the former R-4 reaction. Note that H_2O (v) and H_2 (g) were also included as part of reactions R-1, R-2, R-10 and R-12. In this Table 1 the power law ($k = A \cdot \exp(-E_a/RT)$) kinetic parameters and the rate of the reactions (-r) are also given.

3. Results and discussion

3.1. Thermodynamic model

Thermodynamic prediction model results at temperatures between 500 and 1200 °C are included in Fig. 3, where the outlet composition of vapours, gases and solid carbon of the treatment reactor is shown in weight and volume percentage. The weight percentage results show the distribution of the final products, including the solid carbon that would be formed in the reactor. The volume percentage results, on the other hand, show the composition of what would be the outlet vapour and gas stream, which obviously does not include the solid carbon. Numeric results are included in Supplementary Information (Table S8 and S9). The main highlight is that although a very complex mixture of vapours and gases entered the reactor (specified in Table S8 and S9 and depicted in Fig. 3 as "Inlet"), the mixture simplified into C (s), N_2 (g), H_2 (g), CO_2 (g), CO (g), CH_4 (g), H_2S (g) and H_2O (v), even at the lowest temperature. This means that the hazardousness related to the inlet composition to the treatment reactor would be reduced to the minimum. It could be appreciated that when temperature increased, the amount of C (s), H_2O (v), CO_2 (g) and CH_4 (g) decreased, whereas CO (g) and H_2 (g) increased. The decrease in water content means that the gases generated at 900 °C, and above, would no longer contain condensate, as the partial pressure of water (the only condensable substance) in this gas mixture would be lower than its vapour pressure at room temperature. Additionally, it seems that the system stabilized above 1000 °C, with no further big difference in composition, comprising 31/66 vol% for CO (g)/H_2 (g) with traces of N_2 (g) and H_2S (g), which are the minimum free energy chemicals of the families of nitrogenous and sulphur compounds, respectively, between those defined for the simulation. Regarding the comparison between these results and the experimentally obtained ones (at 700 °C and 900 °C), experimentally higher amount of organic compounds were obtained, what gives an idea of the difference between the real operation and the thermodynamic equilibrium. In any case, the same trend was also observed in the experimental results with regard to

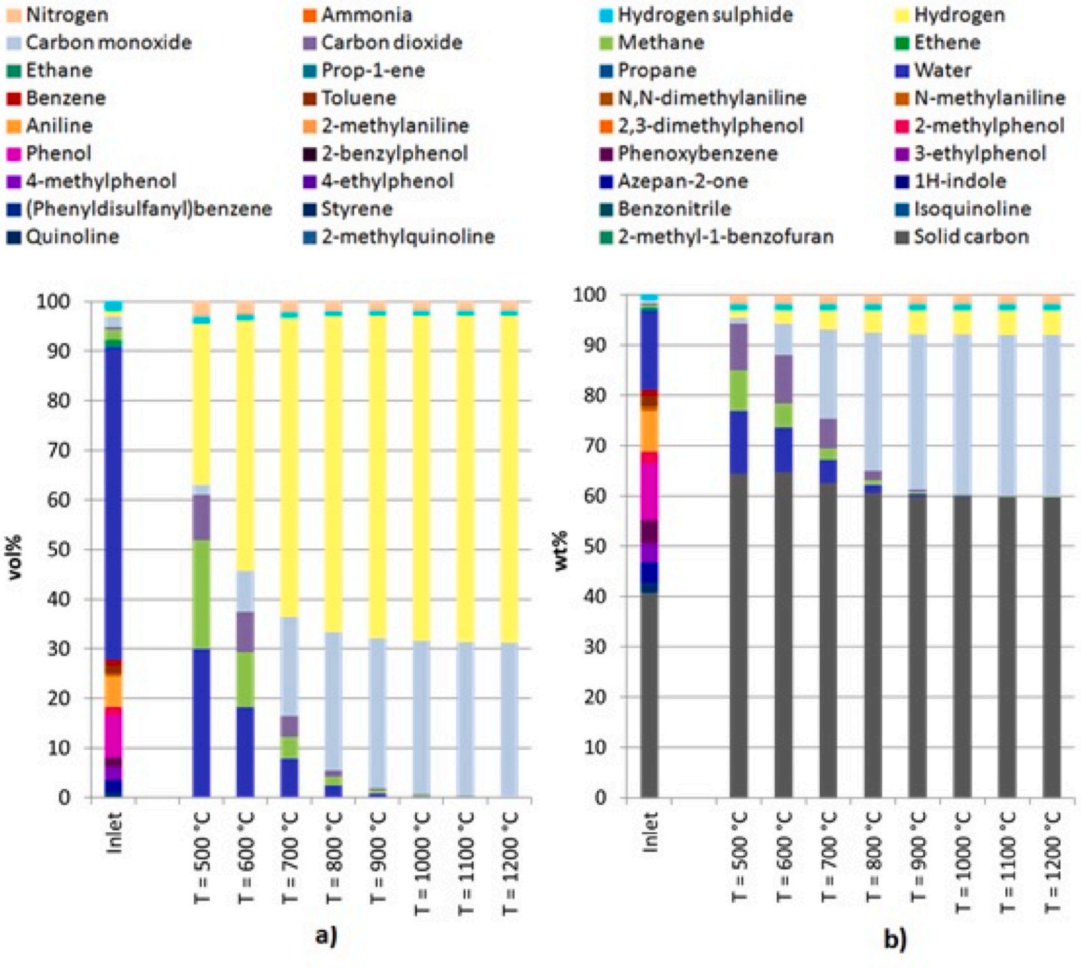

Fig. 3. Pyrolysis vapours and gases outlet composition results for Thermodynamic simulation at temperatures between 500 °C and 1200 °C and 1 bar absolute pressure: a) vol% and b) wt%.

the influence of temperature. At 900 °C, higher amounts of H_2 (g) and CO (g) were observed to the detriment of the organic and water content compared to those registered at 700 °C. Comments related to the C (s) values are discussed in the next section, combined with kinetic simulation results.

Based on the reaction scheme typically used to represent waste gasification processes (Arena, 2012), some extrapolation could be done for pyrolysis reaction mechanisms in order to try to infer the possible reaction mechanism lying behind the thermodynamic results obtained. Taking into consideration the complex nature of the pyrolysis vapours and gases inlet composition and the high temperature of the upgrading process in the treatment reactor, it could be expected that endothermic decomposition reactions for hydrocarbons $pC_xH_y \rightarrow qC_nH_m + rH_2$ and tars $C_nH_m \rightarrow nC + (m/2)H_2$ were occurring. This fact implies that simpler compounds were generated due to breaking of complex organic molecules, as well as carbonization and dehydrogenation reactions. Indeed, at the inlet of the upgrading process, minimal H_2 (g) was present, and therefore, the higher the temperature the more these equilibrium reactions were shifted to the products due to their endothermic nature. Furthermore, the presence of water in the pyrolysis vapours and gases inlet stream enables an additional path for the generation of H_2 (g) and CO (g) through steam reforming reaction $C_nH_m + nH_2O \longleftrightarrow nCO + (n + m/2)H_2$. Even though carbon monoxide was present at the inlet stream, it might prevail the endothermic nature of this later reaction so as to reduce water vapour in favour of CO (g) and H_2 (g) production. According to the observed tendency with temperature increase, where C (s), H_2O (v), CO_2 (g) and CH_4 (g) decrease, additional reactions such as methane steam reforming $CH_4 + H_2O \longleftrightarrow CO + 3H_2$, dry reforming $C_nH_m + nCO_2 \longleftrightarrow 2nCO + (m/2)H_2$ and Boudouard $C + CO_2 \longleftrightarrow 2CO$ could also be occurring. Finally, regarding the nitrogen and sulphur heteroatoms present in the inlet stream, it seems that they evolve into their simplest forms, H_2S (g) and N_2 (g), no matter the operating temperature.

3.2. Kinetic multi-reaction model

The outlet composition of vapours, gases and solid carbon in volume and weight percentage for the fixed bed treatment reactor kinetic simulation is shown in Fig. 4. Numeric results are included in SI (Table S10 to S15). More precisely, results obtained for three operating temperatures (700 °C, 800 °C and 900 °C), considering them as both constant, along the treatment reactor (T_{ct}), and variable, applying the experimentally measured temperature profile (T_{vble}), are shown. In addition, this temperature study was analised for three simulated pressure drop scenarios ($\Delta P = 0$ bar, 1 bar and 2 bar). It is necessary to remember that in the kinetic case, the compounds that will appear as part of the products are only those included in Table 1 as a consequence of the list of reactions defined. This means that the simulator could predict the occurrence of some substances that were not observed experimentally.

As also observed in the thermodynamic prediction, the higher the operating temperature the simpler the generated products for a specific pressure drop. Indeed, less water, toluene, pyrrole, and solid carbon were generated and more benzene, hydrogen cyanide, acetylene, methane, carbon dioxide, carbon monoxide and hydrogen were produced at both studied temperature scenarios (constant and variable),

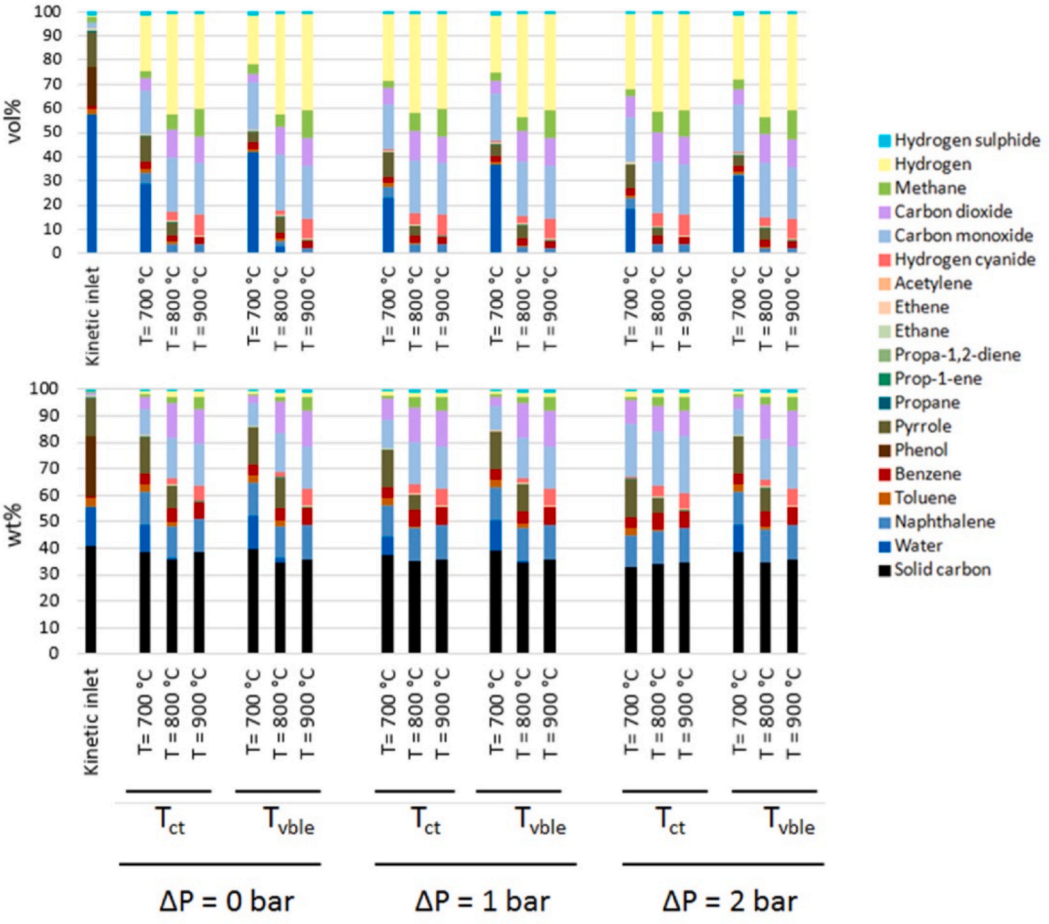

Fig. 4. Kinetic multi-reaction model Simulation outlet Pyrolysis vapours and gases composition in vol% (top) and in wt% (down) in function of temperature (constant and variable at 700 °C, 800 °C and 900 °C) and pressure DROP (0 bar, 1 bar AND 2 bar).

although the effect was maximized at the constant. This can be due to the fact that chemical compounds were kept for longer time at high temperature inside the reactor. Also, a constant quantity of naphthalene was predicted for all the studied conditions, meaning that based on the kinetic parameters associated to the thermal degradation reaction R-11, this compound remains stable. Regarding the prediction of HCN (g) generation, it was not experimentally detected. Therefore, further research would focus on checking its presence as a thermal degradation product of nitrogenous aromatic compounds. Likewise, C_2H_2 (g) is kinetically predicted to be generated and detected experimentally by GC-TCD/FID at 900 °C, although no quantification was possible. Finally, even though predictions could correspond to reality, it could also happen that HCN (g) and C_2H_2 (g) would decompose into simpler species such as C (s), N_2 (g) and H_2 (g) as predicted by the thermodynamic model. However, the kinetic multi-reaction model would not be able to predict the generation of compounds that are not already present in the considered kinetic reactions as products.

Related to the effect of the pressure drop along the treatment reactor ($\Delta P = 0$ bar, $\Delta P = 1$ bar and $\Delta P = 2$ bar), equivalent trend to that described for a temperature increase at constant pressure was observed. Besides, the higher the pressure-drop, the higher the residence time (Table S16). Indeed, longer time inside the reactor seemed to be directly related with a higher amount of heavy organic compounds evolving into lighter ones. In this sense, the effect of temperature would provoke the opposite effect on the residence time. A temperature increase would mean the amount of generated moles increases as endothermic reactions are kinetically and thermodynamically favoured (see defined reaction stoichiometry in Table 1). Therefore, as the reactor volume remained constant, the generated products would pass through the reactor faster.

Regarding the influence of the temperature gradient along the fixed bed treatment reactor, based on the profile of each compound along the treatment reactor (Figure S8), with variable temperature the compounds started reacting at inner positions and stopped earlier too, compared to operations at constant temperature. Not only the temperature is responsible for this difference, but also the concentration at which compounds are present and are available to each other.

Following the kinetic multi-reaction model results of the principal compounds are analysed one by one. These results are discussed comparing them with the previous thermodynamic simulation results and the experimental data. The experimental and kinetic results comparison is depicted in Figure S9 and absolute error of the compounds considered for model validation are given in Table S17.

Solid carbon: at $\Delta P = 0$ bar results show decreasing tendency with a temperature increase at 700 °C and 900 °C, respectively. Thermodynamic (62.7 wt% and 59.9 wt%), kinetic (T vble: 39.5 wt% and 35.7 wt%) and experimental (42.1 wt% and 37.1 wt%). However, kinetically for the T ct scenario, it could be assumed as practically constant (38.6 wt% and 38.8 wt%), although when pressure drop was increased (e.g. $\Delta P = 2$ bar), it slightly increased (33 wt% and 35 wt%). This fact could be explained because at higher pressure drops and temperatures, it seems there is not enough water vapour available (0 wt% and 0 wt%) to continue carrying out the carbon gasification reaction (see R-12 in Table 1) and, therefore, carbonization reactions prevail in the overall effect. Regarding experimental results, the presence of carbonaceous deposition over the fixed bed material was determined from the fixed bed material characterization results and the generated char in the batch reactor from experimental yield calculations. According to the analytical results and experimental observations, compounds such as organic aromatics, solid carbon, sulphur compounds and water vapour, could deposit over the fixed bed material during the pyrolysis vapours and gases upgrading process.

Water vapour: thermodynamic (4.5 wt% and 0.5 wt%), kinetic (T ct: 10.3 wt% and 0.0 wt%; T vble: 12.7 wt% and 0.0 wt%) and experimental (3.9 wt% and 3.7 wt%) results show decreasing tendency with a temperature increase (at 700 °C and 900 °C, respectively) at $\Delta P = 0$ bar. It seems that carbon gasification with steam had significant responsibility on water consumption, as a consequence of the solid carbon present in the reactors. Indeed, the higher the temperature the higher the consumed solid carbon and water vapour quantity. However, experimentally no such big difference was observed between 700 °C and 900 °C compared to the simulation models. This overestimation could be explained by the steady state model assumption, as experimentally could happen that part of the generated water exits the reactor prior to interact with other compounds.

Naphthalene and benzene: in this case thermodynamic simulation and experimental results appear consistent as none of them show naphthalene or benzene as products, while kinetic model results show that once generated it might be hard to decompose them due to their thermal stability. In this regard, although none of these compounds were detected experimentally at 700 °C and 900 °C, further experimental research could be needed as the fraction labelled as *non-recoverable condensed vapours* (Figure S2 and Figure S5) could correspond with those heavier compounds.

Hydrogen gas: thermodynamic (3.9 wt% and 4.8 wt%), kinetic (T ct: 0.9 wt% and 2.1 wt%; T vble: 0.7 wt% and 2.1 wt%) and experimental (0.4 wt% and 2.0 wt%) results show increasing tendency with a temperature increase (at 700 °C and 900 °C, respectively) at $\Delta P = 0$ bar. Indeed, kinetic predictions fit very well the experimental data. Kinetically, the generation of hydrogen was minimal (0.7 wt%) at the lowest temperature (700 °C, simulated as variable) and zero pressure drop, while maxim (2.2 wt%) at the highest temperature (900 °C, simulated as constant) and a pressure drop of 2 bar.

Carbon monoxide, carbon dioxide and methane: thermodynamically CO increased while CO_2 and CH_4 decreased. However, kinetically and experimentally, the two latter also showed increasing tendency with temperature. Kinetic results could be explained due to the fact that no dry reforming of methane reaction (CH_4 (g) + CO_2 (g) → 2CO (g) + $2H_2$ (g)) was considered in the kinetic model. Whereas experimentally, it could occur that in the absence of an adequate catalyst, this reaction could be hardly occurring. Therefore, results at $\Delta P = 0$ bar and at 700 °C and 900 °C, respectively for CO (g), CO_2 (g) and CH_4 (g) are consistent (CO: kinetic T ct: 9.9 wt% and 15.5 wt%; kinetic T vble: 8.7 wt% and 16.2 wt%; experimental: 4.9 wt% and 9.9 wt%. CO_2 (g): kinetic T ct: 4.6 wt% and 12.9 wt%; kinetic T vble: 2.4 wt% and 13.4 wt%; experimental: 7.7 wt% and 9.2 wt%. CH_4 (g): kinetic T ct: 1.0 wt% and 4.8 wt%; kinetic T vble: 5.0 wt%; experimental: 4.1 wt% and 6.2 wt%).

Nitrogen gas: thermodynamic prediction suggested the generation of N_2 (g) while kinetic model did not because none of the decomposition reactions included it as final product. In this regard, based on the consulted literature, typical decomposition species for nitrogenous aromatic compounds seemed to be related to HCN (g), NH_3 (g) and nitrogen oxides (N_2O (g), NO_x (g)) among others. About experimental results, traces of N_2O (g) and NH_3 (g) were identified (section 2.1), which is consistent with the thermal degradation analysis carried out by P. Tranchard to a carbon-reinforced epoxy laminate (Tranchard et al., 2017a). While regarding HCN (g) compound, further experimental research is required in order to determine if this compound is being produced.

Hydrogen sulphide gas: thermodynamic prediction suggested the generation of H_2S (g) while kinetic model did not because none of the decomposition reactions included it as final product, due to the reasons stated in section 2.2. Related to experimental results it seemed that H_2S (g) decreased with increasing temperature (6.5 wt% at 700 °C and 2.6 wt% at 900 °C), which is consistent with the higher amount of sulphur deposited along the fixed bed material at 900 °C compared to 700 °C (see Table S7 in SI).

4. Conclusions

An equilibrium and kinetic multi-reaction model was developed in Aspen Plus software to predict the generation of gaseous outlet stream in function of process parameters (T, P and basic reactor dimensions) for the upgrading process of the vapours and gases generated during the

recycling process of an expired epoxy pre-impregnated composite from the aeronautics industry by pyrolysis. Results show that the system tends to form lighter chemical compounds if enough time and temperature is provided. Even though thermodynamically the process is disfavoured by a pressure increase, kinetically, the rate of the reaction is proportional to the partial pressure of the compounds, and it appears that this effect prevails. Kinetic multi-reaction model is consistent with experimental data at 700 °C and 900 °C at $\Delta P = 0$ bar regarding the generation tendency (in wt%) for the gaseous outcome compounds and water vapour. Solid carbon shows slight differences that could be explained due to the faster water depletion. Indeed, H_2 (g), CO (g), CO_2 (g) and CH_4 (g) increase while water vapour decreases. The lowest absolute error is obtained for H_2 (g) (0.5 wt% at T ct and 0.3 wt% at T vble), while H_2O (v) (6.4 wt% at T ct and 8.8 wt% at T vble) showed the highest. It is concluded that the developed kinetic model sets the base case scenario to assist in a subsequent process upscale optimisation design, in terms of maximising hydrogen gas production, taking into account fluid dynamics and heat transfer phenomena.

Author contribution

Serras-Malillos A.: conceptualization, Methodology, Software, Validation, Formal analysis, Investigation, Writing – original draft, visualisation. Acha E.: conceptualization, Methodology, Investigation, Resources, Writing – review & editing, Supervision, Project administration, Funding acquisition. Lopez-Urionabarrenechea A.: conceptualization, Methodology, Resources, Writing – review & editing, Supervision, Project administration, Funding acquisition. Perez-Martinez B.B.: Validation, Investigation. Caballero B.M.: Resources, Writing – review & editing, Supervision, Project administration, Funding acquisition.

Declaration of competing interest

The authors declare that they have no known competing financial interests or personal relationships that could have appeared to influence the work reported in this paper.

Acknowledgements

The authors want to thank the Ministry of Science and Innovation of Spain (Ref. PID2019-110770RB-I00) and the Basque Government (Ref. KK-2020/00107, ELKARTEK program) for the funding to carry out the investigation. The authors also thank the financing granted to the "Sustainable Process Engineering" research group for the 2016–2021 period (Basque Government, Ref. IT993-16) and are grateful to Iñaki Múgica from Su Medioambiente (SUMA Soluciones Medioambientales, S.L.) for the technical support provided.

Appendix A. Supplementary data

Supplementary data to this article can be found online at https://doi.org/10.1016/j.chemosphere.2022.134499.

References

Abdelouahed, L., Authier, O., Mauviel, G., Corriou, J.P., Verdier, G., Dufour, A., 2012. Detailed modeling of biomass gasification in dual fluidized bed reactors under aspen plus. Energy Fuel. 26, 3840–3855. https://doi.org/10.1021/ef300411k.

Ahmed, A.M.A., Salmiaton, A., Choong, T.S.Y., Wan Azlina, W.A.K.G., 2015. Review of kinetic and equilibrium concepts for biomass tar modeling by using Aspen Plus. Renew. Sustain. Energy Rev. 52, 1623–1644. https://doi.org/10.1016/j.rser.2015.07.125.

Arena, U., 2012. Process and technological aspects of municipal solid waste gasification. A review. Waste Manag. 32, 625–639. https://doi.org/10.1016/j.wasman.2011.09.025.

Aspen Technology Inc., 2021. Aspen Plus.

Barbé, P., Martin, R., Perrin, D., Scacchi, G., 1996. Kinetics and modeling of the thermal reaction of propene at 800 K. Part I. Pure propene. Int. J. Chem. Kinet. 28, 829–847. https://doi.org/10.1002/(SICI)1097-4601(1996)28:11<829::AID-KIN5>3.3.CO;2-O.

Basu, P., 2018. Biomass Gasification, Pyrolysis and Torrefaction Practical Design and Theory, third ed. Joe Hayton, London.

Benson, A.M., 1967. Pyrolysis of propane in a shock tube. AIChE J. 13, 903–908. https://doi.org/10.1002/aic.690130517.

Brodsky, A.M., Kalinenko, R.A., Lavrovsky, K.P., 1960. 863. The principles governing high-temperature ethane cracking. J. Chem. Soc. 4443–4454. https://doi.org/10.1039/jr9600004443.

Bruinsma, O.S.L., Tromp, P.J.J., Nolting de, H.J.J.S., Moulijn, J.A., Institute of Chemical Tehnology (Amsterdam), 1988. Gas phase pyrolysis of coal-related aromatic compounds in a coiled tube flow reactor. 2. Heterocyclic compounds, their benzo and dibenzo derivatives. Fuel 67, 334–340. https://doi.org/10.1016/0016-2361(88)90315-8.

Bueno Lopez, A., Lozano Castelló, D., Perucho Sanchez, F., 2017. WO 2017/021574 A1. Procedimiento de recuperación de fibras inorgánicas a temperatura ambiente en materiales compuestos fibra-resina. pct.

Damartzis, T., Michailos, S., Zabaniotou, A., 2012. Energetic assessment of a combined heat and power integrated biomass gasification-internal combustion engine system by using Aspen Plus®. Fuel Process. Technol. 95, 37–44. https://doi.org/10.1016/j.fuproc.2011.11.010.

De Kam, M.J., Vance Morey, R., Tiffany, D.G., 2009. Biomass integrated gasification combined cycle for heat and power at ethanol plants. Energy Convers. Manag. 50, 1682–1690. https://doi.org/10.1016/j.enconman.2009.03.031.

Francois, J., Abdelouahed, L., Mauviel, G., Patisson, F., Mirgaux, O., Rogaume, C., Rogaume, Y., Feidt, M., Dufour, A., 2013. Detailed process modeling of a wood gasification combined heat and power plant. Biomass Bioenergy 51, 68–82. https://doi.org/10.1016/j.biombioe.2013.01.004.

Gao, N., Chen, C., Magdziarz, A., Zhang, L., Quan, C., 2021. Modeling and simulation of pine sawdust gasification considering gas mixture reflux. J. Anal. Appl. Pyrolysis 155. https://doi.org/10.1016/j.jaap.2021.105094.

Gastelu Otazua, N., 2020. Karbono Zuntzezko Material Konposatuen Pirolisi Bidezko Birziklapena. University of the Basque Country (Engineering School of Bilbao).

Grange, N., Tadini, P., Chetehouna, K., Gascoin, N., Reynaud, I., Senave, S., 2018. Determination of thermophysical properties for carbon-reinforced polymer-based composites up to 1000 °C. Thermochim. Acta 659, 157–165. https://doi.org/10.1016/j.tca.2017.11.014.

Hale, J., 2012. Boeing 787 from ground up. Boeing Comer. Aeromagazine 9.

Hannula, I., Kurkela, E., 2012. A parametric modelling study for pressurised steam/O 2-blown fluidised-bed gasification of wood with catalytic reforming. Biomass Bioenergy 38, 58–67. https://doi.org/10.1016/j.biombioe.2011.02.045.

Lefeuvre, A., Garnier, S., Jacquemin, L., Pillain, B., Sonnemann, G., 2017. Anticipating in-use stocks of carbon fiber reinforced polymers and related waste flows generated by the commercial aeronautical sector until 2050. Resour. Conserv. Recycl. 125, 264–272. https://doi.org/10.1016/j.resconrec.2017.06.023.

Lopez-Urionabarrenechea, A., Gastelu, N., Acha, E., Caballero, B.M., de Marco, I., 2021. Production of hydrogen-rich gases in the recycling process of residual carbon fiber reinforced polymers by pyrolysis. Waste Manag. 128, 73–82. https://doi.org/10.1016/j.wasman.2021.04.044.

López Urionabarrenechea, A., De Marco Rodríguez, I., Caballero, B.M., Gastelu Otazua, N., Hernández Sáinz, A., Adrados López de Viñaspre, A., Solar Irazabal, J., 2016. WO 2016/135359 A1. Method for Treating Vapours Generated during the Process for Recovering Carbon Fibres from Composites by Pyrolysis.

Manion, Huie, Levin, Burgess Jr, Orkin, Tsang, McGivern, Hudgens, Knyazev, Atkinson, Chai, Tereza, Lin, Allison, Mallard, Westley, Herron, Hampson, Frizzell, 2013. NIST Chemical Kinetics Database. NIST Standard Reference Database 17, Version 7.0 (Web Version), Release 1.6.8, Data version 2015.09. National Institute of Standards and Technology, Gaithersburg, Maryland, 20899-8320. Web address: https://kinetics.nist.gov/kinetics/.

Marsh, G., 2010. Airbus A350 XWB update. Reinforc Plast 54, 20–24. https://doi.org/10.1016/S0034-3617(10)70212-5.

McKinnon, M.B., Ding, Y., Stoliarov, S.I., Crowley, S., Lyon, R.E., 2017. Pyrolysis model for a carbon fiber/epoxy structural aerospace composite. J. Fire Sci. 35, 36–61. https://doi.org/10.1177/0734904116679422.

Mutlu, Ö.Ç., Zeng, T., 2020. Challenges and opportunities of modeling biomass gasification in aspen plus: a review. Chem. Eng. Technol. 43, 1674–1689. https://doi.org/10.1002/ceat.202000068.

Nilsson, S., Gómez-Barea, A., Fuentes-Cano, D., Ollero, P., 2012. Gasification of biomass and waste in a staged fluidized bed gasifier: modeling and comparison with one-stage units. Fuel 97, 730–740. https://doi.org/10.1016/j.fuel.2012.02.044.

Panopoulos, K.D., Fryda, L.E., Karl, J., Poulou, S., Kakaras, E., 2006. High temperature solid oxide fuel cell integrated with novel allothermal biomass gasification. Part I: modelling and feasibility study. J. Power Sources 159, 570–585. https://doi.org/10.1016/j.jpowsour.2005.12.024.

Rodat, S., Abanades, S., Coulié, J., Flamant, G., 2009. Kinetic modelling of methane decomposition in a tubular solar reactor. Chem. Eng. J. 146, 120–127. https://doi.org/10.1016/j.cej.2008.09.008.

Sadhukhan, J., Zhao, Y., Shah, N., Brandon, N.P., 2010. Performance analysis of integrated biomass gasification fuel cell (BGFC) and biomass gasification combined cycle (BGCC) systems. Chem. Eng. Sci. 65, 1942–1954. https://doi.org/10.1016/j.ces.2009.11.022.

Salisu, J., Gao, N., Quan, C., 2021. Techno-economic assessment of Co-gasification of rice husk and plastic waste as an off-grid power source for small scale rice milling - an aspen plus model. J. Anal. Appl. Pyrolysis 158, 105157. https://doi.org/10.1016/j.jaap.2021.105157.

Stoliarov, S.I., Leventon, I.T., Lyon, R.E., 2014. Two-dimensional model of burning for pyrolyzable solids. Fire Mater. 38 (3), 391–408. https://doi.org/10.1002/fam.2187. In press.

Towell, G.D., Martin, J.J., 1961. Kinetic data from nonisothermal experiments : thermal decomposition of. AIChE J. 7, 693–698.

Tranchard, P., Duquesne, S., Samyn, F., Estèbe, B., Bourbigot, S., 2017a. Kinetic analysis of the thermal decomposition of a carbon fibre-reinforced epoxy resin laminate. J. Anal. Appl. Pyrolysis 126, 14–21. https://doi.org/10.1016/j.jaap.2017.07.002.

Tranchard, P., Samyn, F., Duquesne, S., Estèbe, B., Bourbigot, S., 2017b. Modelling behaviour of a carbon epoxy composite exposed to fire: Part I-Characterisation of thermophysical properties. Materials 10. https://doi.org/10.3390/ma10050494.

Tranchard, P., Samyn, F., Duquesne, S., Estèbe, B., Bourbigot, S., 2017c. Modelling behaviour of a carbon epoxy composite exposed to fire: Part ii-comparison with experimental results. Materials 10. https://doi.org/10.3390/ma10050470.

Tranchard, P., Samyn, F., Duquesne, S., Thomas, M., Estèbe, B., Montès, J.L., Bourbigot, S., 2015. Fire behaviour of carbon fibre epoxy composite for aircraft: novel test bench and experimental study. J. Fire Sci. 33, 247–266. https://doi.org/10.1177/0734904115584093.

Xu, L., Yang, J., Li, Y., Liu, Z., 2004. Behavior of organic sulfur model compounds in pyrolysis under coal-like environment. Fuel Process. Technol. 85, 1013–1024. https://doi.org/10.1016/j.fuproc.2003.11.036.

Zhang, J., Chevali, V.S., Wang, H., Wang, C.H., 2020. Current status of carbon fibre and carbon fibre composites recycling. Compos. B Eng. 193, 108053. https://doi.org/10.1016/j.compositesb.2020.108053.